Macromolecules
Cite This: Macromolecules 2019, 52, 3753−3762
Article
pubs.acs.org/Macromolecules

# Influence of the Interfacial Effect on Polymer Thin-Film Dynamics Scaled by the Distance of Chain Mobility Suppression by the Substrate

Biao Zuo,*[,†] Fengliang Wang,[†] Zhiwei Hao,[†] Haolin He,[†] Shasha Zhang,[†] Rodney D. Priestley,[‡] and Xinping Wang*[,†]

[†]Department of Chemistry, Zhejiang Sci-Tech University, Hangzhou 310018, China
[‡]Department of Chemical and Biological Engineering, Princeton University, Princeton, New Jersey 08544, United States

Supporting Information

**ABSTRACT:** Polymer−substrate interfaces are significant in determining the dynamics of nanoconfined polymers. In this study, an improved understanding of the interfacial effect was gained from the critical distance over which the suppression of interfacial dynamics originating from an interacting substrate propagates. We investigated the effective viscosity of poly(styrene) (PS) thin films with various molecular weights ($M_w$) on phenyl group-modified substrates and characterized the utmost distance ($h_c^*$) of the suppression of chain diffusional dynamics by the substrate. The viscosity of the PS films on the phenyl-modified substrates increased when the film thickness was decreased below a threshold thickness because of the dominant interfacial effect arising from favorable $\pi-\pi$ polymer−substrate interactions. The extent of viscosity enhancement is apparently larger for PS with high $M_w$ on the same substrate. Most importantly, we found that the interface-induced viscosity increases for all samples with various $M_w$ values and substrates can be linearly correlated with the distance over which the suppression of interfacial dynamics extends, which makes it possible to qualitatively evaluate the effectiveness of the interfacial effect.

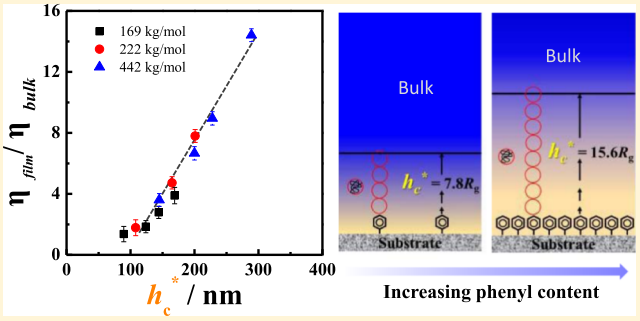


## INTRODUCTION

The molecular mobility of polymers, represented by the glass transition temperature ($T_g$),[1−6] viscosity ($\eta$),[7−10] and diffusion coefficient ($D$)[11−14] of nanoconfined polymers, is substantially affected by the presence of a solid interface because of the possibility of forming various types of interactions between the polymer and substrate. The tremendous alteration of confined polymer dynamics because of the induced interaction at the polymer−substrate interface is generally known as the interfacial effect. From 1994 to 2010, efforts were mainly directed toward elucidating the effect of interfacial interactions on the molecular dynamics of thin polymer films.[15−18] A simplified picture has thus emerged to account for the role of the substrate interface; that is, decreased mobility is observed for polymer films on an attractive substrate, while films supported by a neutral or repulsive substrate are associated with enhanced mobility.[19−22] For example, $T_g$ was depressed for poly(methyl methacrylate) (PMMA) films on a weak interacting substrate (e.g., gold); however, an increasing trend was observed for PMMA on a hydrogen-bonded substrate (e.g., $SiO_x$).[15] In the last five to ten years, knowledge about the interfacial effect has increased, and a large number of experimental results that are seemingly inconsistent with previous conceptions have been reported. Napolitano,[23−26] Koga[27] and Fakhraai[28] et al. found that polymer mobility can also be depressed for polymer films supported by a neutral or repulsive substrate, such as poly(styrene) (PS)/$SiO_x$ systems, provided that sufficient annealing is applied. In contrast, Kumar and Sokolov[29−31] reported that the $T_g$ values of polymer nanocomposites [e.g., poly(2-vinylpyridine); P2VP] were unexpectedly unaffected by the presence of strongly interacting silica nanoparticles. Even for polymer films on an athermal substrate, in which the polymer−substrate enthalpic interaction is counteracted by polymer−polymer cohesion, both positive and negative $T_g$ shifts in the polymer films were observed, depending on the density and molecular weight of the grafted chains.[5,32−34] Additionally, the molecular weight ($M_w$) of the polymer,[35−39] sample preparation,[24,40−43] and curvature of the substrate[44,45] have been revealed to be effective in altering the interfacial effect. Evaluating the extremely complex influences the substrate has on confined dynamics is still a challenge.

The understanding of the interfacial effect has been improved by recent findings on the irreversibly adsorbed

Received: January 31, 2019
Revised: March 25, 2019
Published: May 8, 2019







DOI: 10.1021/acs.macromol.9b00226
Macromolecules 2019, 52, 3753−3762

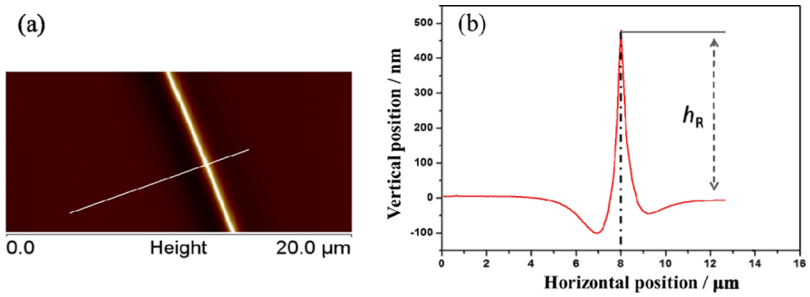


**Figure 1.** (a) Atomic force microscopy (AFM) topological image showing the wetting ridge formed on a 390 nm PS film (442 kg/mol) by placement of $[EIM]BF_4$ droplets on the film surface for 10 min at 160 °C; (b) cross-sectional profile of the area indicated by the white line in panel (a).

layer and the propagation of interfacial dynamics. Polymer chains can be firmly adsorbed on even a neutral substrate to form an immobilized adsorbed layer.[42,46−48] The severely suppressed mobility of interfacial adsorbed chains can extend up to tens of $R_g$ (radius of gyration) and eventually counteract the enhanced mobility at the free surface,[49−54] therefore dominating the thin-film dynamics. As suggested by Napolitano,[54] Cangialosi,[54] and Wang,[53] the changes in a state of chain adsorption can induce large variations in the depth over which the suppressed dynamics can extend, and therefore, the effect of the substrate interface on the chain mobility, measured under confinement, is directly related to the degree of chain adsorption on the substrate. These results suggest that how significantly the substrate influences molecular mobility does not simply depend on the polymer−substrate interaction but essentially on the strength of chain adsorption on the substrate and, by extension, on the propagation distance of the suppressed interfacial dynamics due to chain adsorption. However, unfortunately, due to the lack of systematic characterization of the distance of polymer dynamics suppression by a substrate, the relationship between the confined dynamics of thin films dominated by the interfacial effect and the length scale of interfacial dynamics suppression has not yet been disclosed.

In our previous work, we developed a method based on measuring the vertical diffusion of fluorinated tracer-labeled polymer chains in a bilayer film to assess the utmost distance from a substrate over which polymer dynamics are suppressed.[55] Meanwhile, the effective viscosity—a measure of chain mobility—of supported polymer thin films can be acquired by probing the growth dynamics of the "*wetting ridge*" formed on the films' surface due to the vertical component of surface tension of the liquid droplet atop the film surface, as previously reported.[56] We herein characterized these two aspects of the properties of PS thin films supported by an attractive substrate and investigated how these aspects are correlated. We chose PS with various $M_w$ values as a model polymer and $SiO_x$ covered by various amounts of phenyl groups as a substrate to construct a series of polymer−substrate combinations with tunable interfacial interactions. The results showed that the viscosity of PS thin films changed significantly with both the $M_w$ of PS and substrate surface chemistry, and furthermore, all of the data on viscosity variations can be linearly scaled by the propagation depth of the suppression of interfacial dynamics.

## EXPERIMENTAL SECTION

**Materials.** Monodispersed PS (PDI = 1.05−1.18) with various $M_w$ values was purchased from Polymer Source Inc. (Canada). PS end-capped with 2-perfluorooctylethyl methacrylate (FMA) units ($PS_{260}$-*ec*-$FMA_1$, PDI = 1.13; $PS_{428}$-*ec*-$FMA_2$, PDI = 1.15; and $PS_{682}$-*ec*-$FMA_2$, PDI = 1.18, where the subscript is the degree of polymerization) was synthesized using atom-transfer radical polymerization (ATRP), as described in previous work.[57,58] Phenyltrimethoxysilane ($C_6H_5Si(OCH_3)_3$, PTS) was purchased from Aldrich Co. (USA). 1-Ethyl-3-methylimidazolium tetrafluoroborate ($[EIM]BF_4$) (surface tension: 51 mN/m) was supplied by the Lanzhou Institute of Chemical Physics, Chinese Academy of Sciences.

**Preparation of the Substrates.** Native oxide-covered silicon wafers ($SiO_x$/Si) were prepared by immersing a silicon wafer (100) into a piranha solution consisting of $H_2SO_4/H_2O_2$ (3:1) for 20 min at 90 °C. The wafer was then rinsed in deionized water and dried under a nitrogen atmosphere. The thickness of the $SiO_x$ layer was ∼2.0 nm.

The phenyl group-modified substrate was prepared following the reported method.[16,59] PTS was grafted onto the $SiO_x$/Si surface by exposure of the cleaned wafer to the PTS solution in anhydrous toluene for various times. The phenyl group-modified substrates were characterized by the water contact angle, X-ray photoelectron spectroscopy (XPS), and sum frequency generation (SFG) spectroscopy. The results are shown in Table S1 and Figure S1, respectively. The fraction of phenyl groups covering the surface can be estimated by using the Cassie equation[16,60,61] on the basis of the water contact angle data (see details in Table S1). Substrates with a phenyl group coverage of 22, 46, and 60%, denoted as PTS-1, PTS-2, and PTS-3, were obtained by immersing the substrate for 17, 40, and 54 min, respectively, in 0.25 vol % PTS solution at 60 °C. A substrate surface with 90% coverage with phenyl groups (PTS-4) was obtained by performing the treatment in 1.0 vol % PTS solution at 60 °C for 1 h.

**Film Formation.** The PS films were fabricated by spin-coating from a toluene solution of the polymer onto clean substrates. The prepared films were annealed at 150 °C for 72 h in a vacuum to remove the residual solvent and stress. Ellipsometry ($EP^3SW$, Accurion Co., Germany) was applied to measure the film thickness.

**Viscosity Determination of the Supported PS Films.** Following our previously reported method,[56] the effective viscosity ($\eta$) of the supported PS films was measured by monitoring the growth of the "wetting ridge"—a microscopic protrusion on the film surface because of the capillary forces exerted by a drop of the ionic liquid placed on the film surface. In measurement, a small volume of $[EIM]BF_4$ was gently deposited onto the PS film surface at temperatures above the bulk $T_g$ ($T_g^{bulk}$), forming a half spherical droplet with a contact angle ($\theta$) of 76°. It was predetermined that $[EIM]BF_4$ cannot swell or plasticize the PS surface.[22,56,62] Under the pulling of the vertical component of the surface tension ($\gamma$) of the ionic liquid droplet ($\gamma_\perp$; $\gamma_\perp = \gamma \sin\theta$), the film surfaces near the three phase line were deformed, and a ridge-like protrusion, called the "wetting ridge", spontaneously formed, as shown in Figure 1. A qualitative analysis of the stress−strain relationship of the deformation process by Shanahan[63,64] shows that the local strain ($\sigma$) can be


DOI: 10.1021/acs.macromol.9b00226
*Macromolecules* 2019, 52, 3753−3762

expressed as a ratio ($\varepsilon = h_R/\omega$) between the height ($h_R$) and width of the wetting ridge ($\omega$); and the stress ($\sigma$) is represented by a ratio, $\sigma = \gamma_\perp/\omega$. In a viscous flow, the strain rate ($\dot{\varepsilon}$) is determined by the ratio of stress ($\sigma$) to viscosity ($\dot{\varepsilon} = \sigma/\eta$). In our case, $\dot{\varepsilon} = h_R/\omega t$, and thus we have $h_R(t) \approx (\gamma \sin \theta/\eta)t$. Accordingly, at a long force acting time (i.e., $t \gg \tau_0$, $\tau_0$ being the terminal relaxation time), $h_R$ is expected to increase linearly with time, with a slope ($k$) proportional to $\gamma \sin \theta/\eta$ ($k = \alpha\gamma \sin \theta/\eta$; $\alpha$ is a correcting factor). This relationship was evidenced by our previous work, and the value of $\alpha$ was estimated to be 0.37 for PS with $M_w$ values from 168 to 1070 kg/mol. Then, we have $\eta = 0.37\gamma \sin \theta/k$.[56] The viscosity of the PS films can be determined by characterizing the rate of wetting ridge growth with time, that is, the value of $k$.

Detailed procedures are described below. A heating stage (INSTEC, USA) with an accuracy of ±1 K was used to control the temperature. After 5 min of preheating the polymer film, a droplet of the ionic liquid with a volume of 4 μL was gently deposited onto the surface of the polymer film and kept for a desired time $t$. Then, the film (with the liquid droplet) was quickly transferred onto the surface of an ice bag to ensure that the wetting ridge was frozen during polymer film cooling. The ionic liquid droplet was removed, the film was rinsed with distilled water, and then, the film was dried under a nitrogen stream. The three-dimensional profiles of the wetting ridge were determined by AFM (Multimode-8, Bruker, USA) at 25 °C. The height of the wetting ridge could be reproducibly determined due to the high vertical resolution of the AFM. The vertical distance between the highest point and the undisturbed flat surface was defined as the height of the wetting ridge ($h_R$; Figure 1b).

**Determination of the Utmost Distance of Polymer Dynamics Suppression by Substrates.** The distance over which chain mobility is suppressed by a solid substrate was measured by detecting the diffusion of fluorinated labeled PS chains in a bilayer film consisting of a 50 ± 2 nm PS top layer and a variable-thickness PS-*ec*-FMA$_n$ ($n$ = 1 or 2) bottom layer supported on the substrate.[55] At $T > T_g^{bulk}$, the fluorinated chains (i.e., PS-*ec*-FMA$_n$) in the bottom layer diffuse through the PS layer on top and eventually reach the free surface of the bilayer film. The critical time ($t^*$) for the fluorinated chains to diffuse from the interface of the bottom layer to the surface of the bilayer film can be obtained by detecting the changes in the water contact angle on the film surface. The value of $t^*$ varied with the thickness of the bottom PS-*ec*-FMA$_n$ layers due to the different extent of influence by the substrate. A threshold thickness of the bottom layer ($h_c^*$), corresponding to the thickness at which $t^*$ starts to increase, can be obtained reliably. $h_c^*$ represents the utmost distance over which the polymer dynamics were altered by the substrate.[55]

The details of the preparation of the bilayer film are described below. The bottom PS-*ec*-FMA$_n$ layer was prepared by spin-coating a toluene solution of the polymer onto the substrate surface. The film was then annealed at 150 °C under vacuum for 24 h to remove the residual solvent and to promote the segregation of FMA end units onto the surface. The upper PS layer, with almost the same $M_w$, was prepared by a water-casting method[65] from toluene solution on a distilled water surface and then picked up by the PS-*ec*-FMA$_n$-coated substrate. The bilayer film was then dried under vacuum at 60 °C for 72 h to remove the residual solvent and water trapped between the layers.

## RESULTS AND DISCUSSION

**Effective Viscosity of Supported PS Thin Films.** The effective viscosity of the PS thin films ($\eta_{film}$) on the phenyl group-modified substrates was assessed by detecting the time evolution of the height of the wetting ridge ($h_R$) using AFM. Figure 1 presents a representative AFM topological image of the wetting ridge formed on a 390 nm PS film ($M_w$ = 442 kg/mol), from which $h_R$ can be reliably determined. In addition to the protruding ridge itself, dimples are clearly observed on both sides of the ridge. This profile feature suggests that the wetting ridge was built up because of the flow of polymer chains near the dimple region toward the center and tip of the ridge. Essentially, the kinetics of wetting ridge formation was controlled by the ease of polymer chain flow within the film, which is related to the film viscosity. When the droplet placement time (i.e., force acting time) is longer than the terminal relaxation time of the polymer ($t_0^{bulk}$; $t_0^{bulk} \approx 100$ s for PS with $M_w$ = 442 kg/mol at 160 °C[66]), $h_R$ increases linearly with time, as shown in Figure 2. On the basis of scaling analysis

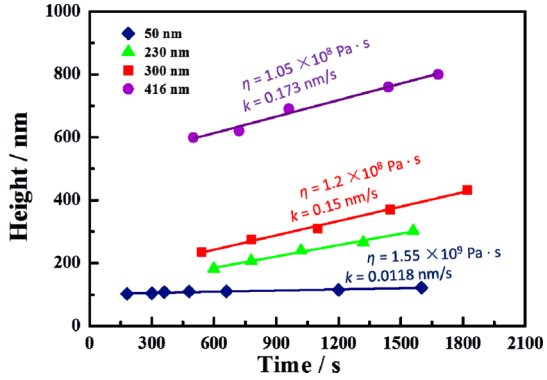


**Figure 2.** Height of the wetting ridge ($h_R$) as a function of the droplet deposition time for PS films ($M_w$ = 442 kg/mol) with various film thicknesses. PTS-4 was used as a substrate ($T$ = 160 °C).

of the stress−strain correlation, in which $\sigma = \gamma \sin \theta/\omega$ and $\dot{\varepsilon} = h_R/\omega t$, the viscosity of the film can be deduced from the slope $k$, in that $\dot{\varepsilon} = \sigma/\eta$, which gives $k = \alpha\gamma \sin \theta/\eta$ for the response of the viscous flow.[56] The $\eta_{film}$ of PS on the PTS-modified substrate can be calculated from the slope $k$ (Figure 2) on the basis of the predetermined values of $\gamma$ ($\gamma$ = 51 mN/m for [EIM]BF$_4$), $\theta$ ($\theta$ = 73°), and $\alpha$ ($\alpha$ = 0.37).[56] Herein, the deduced viscosities of the 390 and 416 nm thick PS films, in which the ultrathinning effect is absent,[67,68] are within the same order of magnitude as the value for bulk PS with a similar $M_w$ ($\eta_{PS}$ = 5.9 × 10$^7$ Pa·s at 160 °C).[69]

The $\eta_{film}$ values of PS ($M_w$ = 442 kg/mol) with various film thicknesses on bare SiO$_x$ and on the phenyl group-modified substrates were measured using the *"wetting ridge growth"* method (see results in Figure 3). For films on bare SiO$_x$, in line with the literature results,[70] $\eta_{film}$ decreases monotonically with decreasing film thickness ($h$) for films with $h$ < 130 nm. The 50 nm thick PS film exhibits a twofold reduction in bulk viscosity

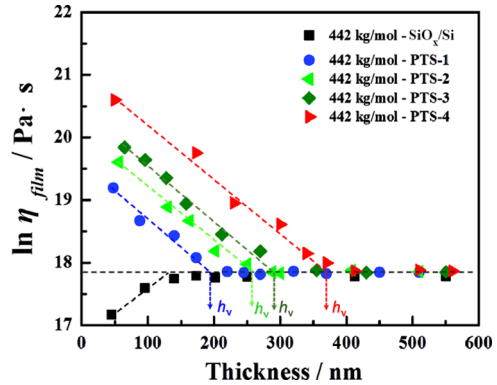


**Figure 3.** Plot of viscosity against film thickness of PS films with $M_w$ = 442 kg/mol supported by substrates with various phenyl group contents. $T$ = 160 °C.



DOI: 10.1021/acs.macromol.9b00226
Macromolecules 2019, 52, 3753−3762

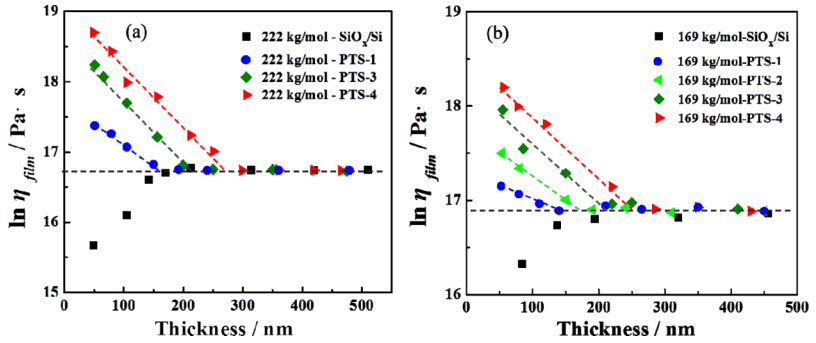


**Figure 4.** Plots of viscosity against film thickness of PS films with a $M_w$ of (a) 222 and (b) 169 kg/mol supported by substrates with various phenyl group contents. $T$ = 145 and 160 °C for PS with $M_w$ = 169 and 222 kg/mol, respectively.

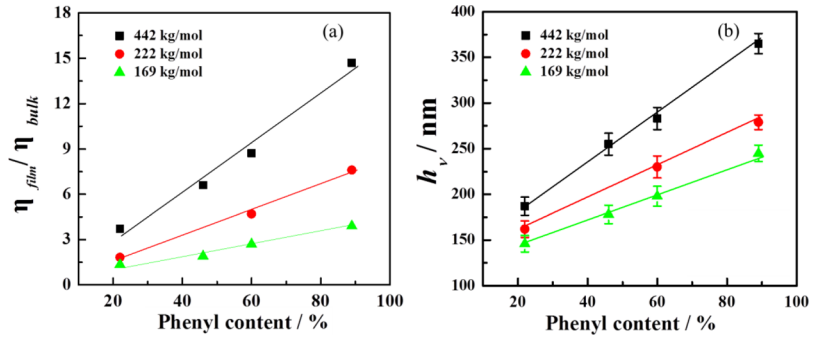


**Figure 5.** (a) Normalized viscosity ($\eta_{film}/\eta_{bulk}$) of the 50 nm PS film and (b) $h_v$ as a function of the phenyl group content on the substrate surface. ($T$ = 160 °C for PS with $M_w$ = 222 and 442 kg/mol; $T$ = 145 °C for PS with $M_w$ = 169 kg/mol).

($\eta_{bulk}$). Note that, at the same film thickness, the drop in viscosity of the PS-on-$SiO_x$ system is limited to one order of magnitude,[8,70−72] and our data are in agreement with these results.[70] However, in contrast, $\eta_{film}$ exhibits an increasing trend with a reduction in film thickness when PTS-modified $SiO_x$ was used as the supporting substrate. Specifically, at $h$ = 50 nm, the $\eta_{film}$ of PS films on the PTS-4 substrate is approximately 15-fold larger than $\eta_{bulk}$, indicative of the highly sluggish chain mobility. Moreover, the increase in viscosity is greater, and the threshold film thickness ($h_v$, Figure 3), where $\eta_{film}$ starts to increase, becomes larger for films supported by a substrate covered with a larger amount of phenyl groups. This result means that the mobility of PS chains in thin films was significantly depressed by introducing phenyl groups on the substrate surface.

An increase in viscosity upon confinement is usually found in systems with strong polymer−substrate interactions.[56,73−75] In our case, interfacial $\pi-\pi$ interactions are supposed as the main reason for the increased viscosity of PS films on phenyl-modified substrates. In our previous work,[61] $\pi-\pi$ interactions at the interface of a polystyrene/phenyl-functionalized substrate were identified by SFG spectroscopy. Spectral analysis showed that the PTS phenyl groups on the $SiO_x$ surface induced the perpendicular orientation of PS phenyl rings by energetically favorable parallel-displaced $\pi-\pi$ interactions at the interface. The PS chains were pinned flat on the substrate surface, and significantly slower dynamics of PS chains at the interface and in the thin film resulted because of the $\pi-\pi$ interactions between the chains and substrate. Therefore, it is reasonable that the increased viscosity of PS films on PTS-modified substrates is because of the adsorption of chains at the interface facilitated by the interfacial $\pi-\pi$ interactions formed between the phenyl groups on the substrate surface and those in PS chains.

The effect of the presence of an interacting substrate on the viscosity of PS films, that is, the interfacial effect, depends on the $M_w$ of PS. Viscosities of thin PS films with $M_w$ of 222 and 169 kg/mol are shown in Figure 5. Note that because the wetting ridge for low viscosity PS with a $M_w$ of 169 kg/mol grew so rapidly at 160 °C that we could not obtain a reliable $h \approx t$ curve,[56] the viscosity of this low $M_w$ sample was measured at a lowered temperature of 145 °C. Comparing the data for PS with $M_w$ values of 169, 222 (Figure 4), and 442 kg/mol (Figure 3), we found that both the rise in $\eta_{film}$ with respect to $\eta_{bulk}$ and the $h_v$ values were considerably larger for PS films with a higher $M_w$. The $M_w$ effect can be visualized clearly in Figure 5, which displays the normalized viscosity ($\eta_{film}/\eta_{bulk}$)—a parameter reflecting the extent of the increase in viscosity caused by the PTS-modified substrate—of the 50 nm thick PS films and $h_v$ as a function of the phenyl content on the substrate. PS films with a higher $M_w$ exhibit a larger $\eta_{film}/\eta_{bulk}$ and $h_v$. Meanwhile, $\eta_{film}/\eta_{bulk}$ and $h_v$ increase more rapidly with the content of phenyl groups for films with larger $M_w$. These data demonstrate that the mobility of chains with a larger $M_w$ in a film was more severely suppressed by the substrate, indicative of a stronger interfacial effect.

Taking into account all the above results, the decrease in chain mobility because of the interacting substrate is more pronounced for PS films supported by a more strongly interacting substrate and for films with a larger $M_w$. In the following discussion, we will show that the changes in chain dynamics of PS thin films due to the interfacial effect can be scaled by the distance over which the suppressed interfacial mobility propagates.



DOI: 10.1021/acs.macromol.9b00226
Macromolecules 2019, 52, 3753−3762

**Utmost Distance of Chain Dynamics Suppression by the Substrate.** It is generally accepted that the suppression of interfacial dynamics can propagate over a long distance from the interface, and as a result, the dynamics of polymer thin films with thicknesses up to hundreds of nanometers can be perturbed by the substrates. Therefore, the distance to which the retarded interfacial mobility propagates is clearly important and could be a critical parameter that changes the dynamics of thin films. Herein, we used a previously published method to detect the utmost distance of PS dynamics suppression by the substrate by investigating the diffusion of a fluorinated tracer-labeled PS chain.[55] The inset of Figure 6a illustrates the sample geometry for the measurement, that is, a bilayer film composed of a bottom layer of PS-*ec*-FMA$_n$ ($n$ = 1 or 2) with the fluorinated components enriched at the upper interface and a 50 nm top PS layer ($h_{up}$). Upon thermal annealing of the bilayer films at 130 °C ($T_g^{bulk}$ + 30 °C), the fluorinated chains diffuse through the top PS layer and eventually come into contact with the free surface. The minimal time required for fluorinated chains to diffuse from the underlying interface to the top of the PS surface ($t^*$) was acquired by detecting the onset of an increased water contact angle due to the hyper-hydrophobic nature of FMA, as shown in Figure 6. Here, it is noticeable that a lower temperature (i.e., 130 °C) than the viscosity experiment (i.e., 145 and 160 °C) had to be chosen in order to ensure the moderate diffusion rate of the fluorinated chains and the experimentally accessible $t^*$ value. We then investigated the variation of $t^*$ with the thickness of the bottom layer ($h_c^*$). A critical bottom film thickness value ($h_c^*$), where $t^*$ starts to increase, was identified by plotting $t^*$ against $h_b$, as shown in Figure 7a. At $h_b < h_c^*$, the $t^*$ value increases as we decrease the $h_b$, because of the increasing impact of the substrate on chain mobility closer to the substrate. In contrast, at $h_b > h_c^*$, the distance between the substrate surface and the PS$_{431}$//PS$_{428}$-*ec*-FMA$_2$ interface is sufficiently long that the substrate did not influence the chain mobility at the interface, leading to unchanged $t^*$ values; Figure 7a. Accordingly, $h_c^*$ could be reasonably regarded as the utmost distance from the substrate of polymer dynamic suppression, as verified previously.[55]

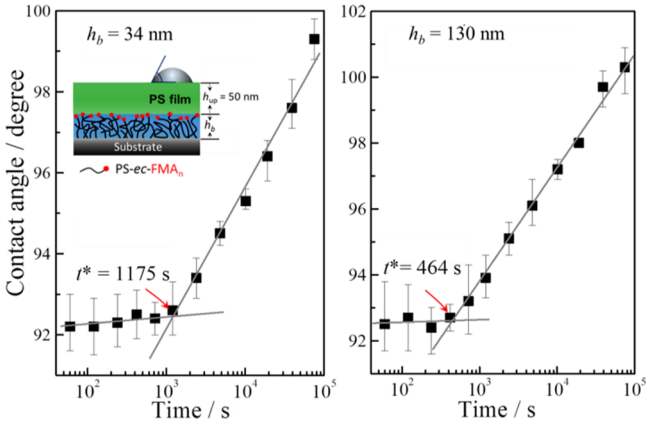


**Figure 6.** Water contact angles ($\theta$) on the surface of a PS$_{431}$//PS$_{428}$-*ec*-FMA$_2$ bilayer film on a PTS-4 substrate as a function of annealing time at 130 °C.

Figure 7b presents $h_c^*$ values for PS with $M_w$ values of 27, 45, and 71 kg/mol on substrates functionalized with phenyl groups. $h_c^*$ increases with increasing phenyl group coverage because of the increased $\pi-\pi$ interactions at the interface. Interestingly, on the same substrate, the value of $h_c^*$ increases with the $M_w$ of the PS film. Additionally, the slope of $h_c^*$ is also larger for PS with a higher $M_w$. The changes in $h_c^*$ with the phenyl content on the substrate surface for PS with different $M_w$ values, shown in Figure 7b, shared a qualitatively similar trend with the variation in $\eta_{film}/\eta_{bulk}$ with the phenyl content depicted in Figure 5. Both the $h_c^*$ and $\eta_{film}/\eta_{bulk}$ values increased with the coverage of phenyl groups on the substrate surface. This might potentially suggest that the effect of the substrate on the chain mobility of polymer thin films is related to how far the suppression of interfacial dynamics can propagate.

The $h_c^*$ value of high-$M_w$ PS cannot be directly measured using the current method because fluorinated tracer-labeled PS with $M_w$ > 150 kg/mol cannot be prepared by ATRP. Instead, it is possible to deduce the $h_c^*$ value for PS with $M_w$ = 169, 222, and 442 kg/mol from those of PS with low $M_w$ because of the unique dependence of $h_c^*$ on $M_w$; that is, the ratio of $h_c^*/R_g$ is usually a constant value. We previously found that $h_c^*/R_g$ = 9.5 for PMMA on a SiO$_x$ substrate; furthermore, Rubinstein et al.[14] revealed that $h_c^*/R_g$ = 10 for PS thin films. In this study, we found that the ratios of $h_c^*/R_g$ were 7.8, 10.1, 13.5, and 15.6 for PS on PTS-1, PTS-2, PTS-3, and PTS-4 substrates, respectively (Figure 8a). The constant $h_c^*/R_g$ values indicate that the suppressed interfacial dynamics was delivered by virtue of the connection of macromolecular chains by topological entanglements, which is in agreement with proposals put forward by Koga et al.[52] Moreover, Rubinstein's results

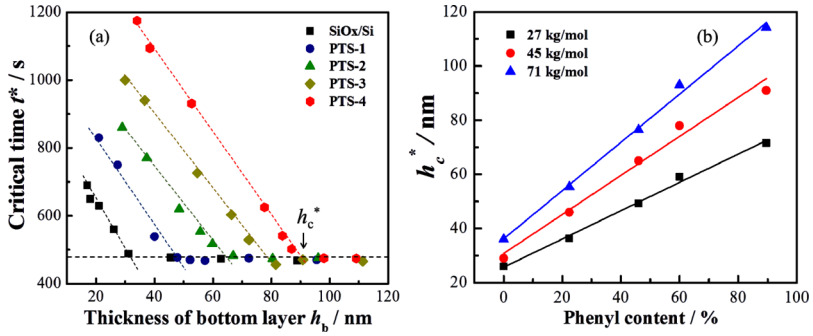


**Figure 7.** (a) Relationship between the critical time ($t^*$) and the thickness of the bottom layer ($h_b$) in bilayer films of PS$_{431}$//PS$_{428}$-*ec*-FMA$_2$ on various substrates. (b) Relationship between $h_c^*$ and the content of phenyl groups on the substrate surface for PS with $M_w$ values of 27, 45, and 71 kg/mol ($T$ = 130 °C).



DOI: 10.1021/acs.macromol.9b00226
*Macromolecules* 2019, 52, 3753−3762

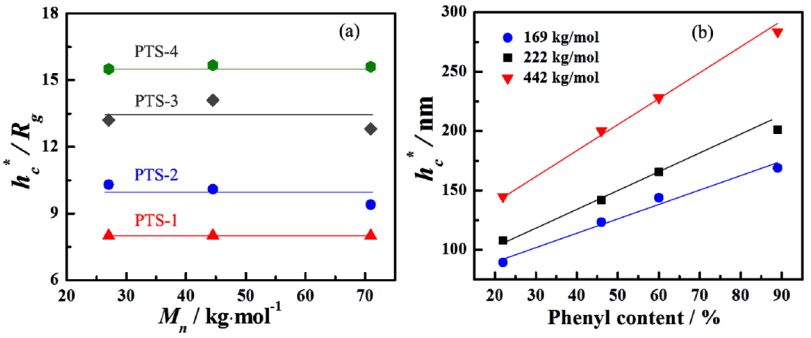


**Figure 8.** (a) $h_c^*/R_g$ as a function of the $M_w$ of PS on the PTS-modified substrate at 130 °C; (b) relationship between $h_c^*$ and the phenyl content on the substrate surface for PS with $M_w$ of 169, 222, and 442 kg/mol.

revealed that the constant $h_c^*/R_g$ holds for PS with $M_w$ values up to 770 kg/mol.[14] Accordingly, $h_c^*$ values for PS films with $M_w$ values of 169, 222, and 442 kg/mol (Figure 8b) were reasonably estimated based on the $h_c^*/R_g$ values shown in Figure 8a. Similar to the results in Figure 7b, the $h_c^*$ for PS films with higher $M_w$ are larger than those with lower $M_w$.

**Influence of the Interfacial Effect on the Mobility of Polymer Thin Films Scaled by the Distance of Dynamics Suppression by the Substrate.** In this section, we correlated the viscosity rise of PS thin films due to the interfacial effect to the distance of dynamics suppression by the substrate. The viscosities of PS films with $M_w$ = 169 kg/mol at 145 °C and that with $M_w$ = 222 and 442 kg/mol at 160 °C were simply converted into the data at 130 °C, where the $h_c^*$ values were determined on the basis of the time−temperature dependent Vogel−Fulcher−Tammann law for bulk PS films determined by our previous work.[56] In Figure 9, we plot $\eta_{film}/\eta_{bulk}$ and $h_v$ against $h_c^*$ for PS thin films on the various substrates and with varying $M_w$ values (i.e., 169, 222, and 422 kg/mol) at a temperature of 130 °C. The $\eta_{film}/\eta_{bulk}$ data for all the samples collapsed into a linear line. This result clearly demonstrated that the interfacial effect on the mobility of thin films can be scaled by the propagation distance of the suppression of interfacial dynamics. Such an assertion can also be supported by the fact that divergences from the linear correlation started to occur at low $\eta_{film}/\eta_{bulk}$ values (i.e., $\eta_{film}/\eta_{bulk}$ < 1.5), where the interfacial effect eventually diminished (Figure 9a). The results provide an additional perspective in understanding the interfacial effects of confined polymers; that is, the effect of the substrate, which varies with $M_w$, the substrate properties, and so forth can be unified by the distance of chain dynamics suppression by the substrate.

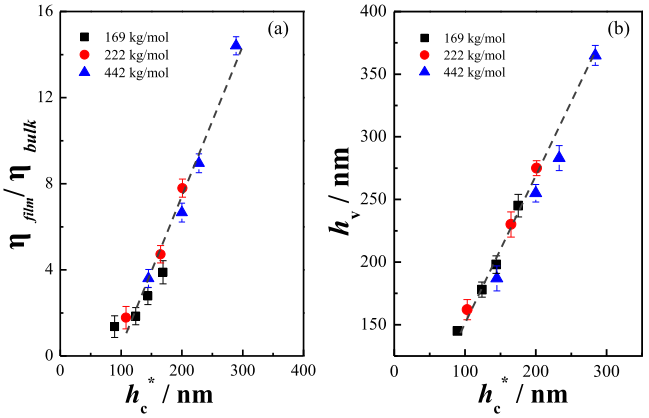


**Figure 9.** Linear correlation between (a) $\eta_{film}/\eta_{bulk}$ for films at $h$ = 50 ± 3 nm and (b) $h_v$ and the distance of polymer dynamics suppression by the substrate ($h_c^*$). $T$ = 130 °C.

The results in Figure 9 can be understood on the basis of the *layer model*,[1,76−78] which is commonly invoked in describing the dynamics of polymer thin films and normally considers thin films as composed of a free surface layer, a bulk layer, and an interfacial layer. The weighted average of chain mobility in the individual layers determines the global dynamics of the film. When the polymer−substrate interaction is strong, such as in the current investigated PS/PTS-modified $SiO_x$ system, the enhanced mobility on the free surface is counteracted by the suppressed interfacial dynamics, resulting in films containing merely bulk and interfacial layers.[53,54] A gradient structure,[27,32,52,79] in which the suppressed interfacial mobility gradually recovers to the bulk value with increasing distance from the supporting interface, can be applied to describe dynamics in the interfacial layer. The chain mobility of a supported film with relatively strong interfacial interactions can be formulized according to the layer model. Taking $T_g$ as an example, we have

$$T_g(h) = \frac{h - h_1}{h} T_g^{bulk} + \frac{\int_0^{h_1} T_g(z)dz}{h} \quad (1)$$

where $h_1$, or alternatively $h_c^*$, is the utmost distance over which the interfacial effect can extend. The second term accounts for the contribution of the interfacial layer, in which $T_g(z)$ is the function describing the depth distribution of the local $T_g$, and the integral ($\int_0^{h_1} T_g(z)dz$) is the sum of $T_g(z)$ for all sublayers with different distances from the supporting interface. It is obvious from eq 1 that two parameters $h_1$ (also $h_c^*$) and $T_g(z)$ are key to the dynamics (e.g., $T_g$ and viscosity) of thin films. An increased distance over which the retarded interfacial dynamics persists (i.e., larger $h_c^*$) is associated with a larger interfacial effect, resulting in significantly slowed thin-film dynamics as the viscosity rises, as presented in Figure 9.

The results in Figure 9, which correlate the effectiveness of the interfacial effect of the polymer with the length scale over which the hindered interfacial mobility propagates, update our understanding of the interfacial effect of polymers. Recently, it has been reported that the mobility of a sufficiently annealed polymer film supported by a neutral or repulsive substrate (e.g., PS on $SiO_x$) can be suppressed,[23−28] but while the dynamics were almost unchanged for polymer nanocomposites with very strong polymer−particle interactions, such as P2VP



DOI: 10.1021/acs.macromol.9b00226
*Macromolecules* 2019, 52, 3753−3762

and silica.[29−31] We note that these seemingly inconsistent findings can be rationalized by exploiting the results of Figure 9. For films on a neutral substrate, the distance over which the interfacial dynamics extend increases with increasing annealing time,[54,55] and thus, if sufficient annealing is applied, the free surface effect can be neutralized by the long-range suppression of the interfacial effect, resulting in decreased film mobility. However, for nanocomposites with very strong polymer−particle interactions, Star et al.[80] proposed that a strongly "bound" polymer layer is adsorbed to the nanoparticle surface and "cloaks" the particles so that the suppression of interfacial dynamics cannot be transmitted into the bulk, as a result of which the polymer dynamics (i.e., thermodynamic $T_g$) are unaffected by the interface. Thus, it is reasonable to propose that the interfacial effect in different nanoconfined systems can be better comprehended when the pathway for interfacial mobility propagation or the gradient in interfacial dynamics are considered. This view is in agreement with the perspective of Star et al.,[81] who stated that "careful measurements of the gradient of relaxation across the film profile are ultimately needed to provide a complete picture of the film dynamics".

Additionally, this study provides an alternative insight into the effect of $M_w$ on the interfacial effect of polymer thin films. In Figure 5, we show that the mobility of PS thin films with higher $M_w$ decreased more substantially than those of films with low $M_w$; moreover, Figures 7b and 8b showed that $h_c^*$ increased with $M_w$. This indicates that a polymer with a larger $M_w$ is more effective in transmitting the suppression of interfacial mobility, resulting in a stronger interfacial effect and greatly depressed film mobility. This concept is in qualitative agreement with the "interfacial slippage" effect proposed by Tsui et al., which suggests that the dynamics of polymer thin films with larger $M_w$ could be more strongly influenced by the presence of a substrate because of the deeper penetration of the interfacial adsorbed chains with depressed mobility into the film interior.[8,72,82] Additionally, the larger number of contacts with the solid substrates made by the chains of larger $M_w$, as evidenced by Simavilla and Napolitano et al.,[83] can also amplify the suppressed interfacial effects because of the enhanced polymer−substrate interactions per chains. However, our results are seemingly inconsistent with the "chain packing" argument proposed by Sokolov et al.[35] for poly(vinyl acetate)/$SiO_2$ and P2VP/$SiO_2$ nanocomposites. In their model, nanocomposites with lower $M_w$ exhibit a more pronounced interfacial effect due to the increased packing efficiency of the low-$M_w$ chains at the interface. We suspected that the different $M_w$ dependence found in our and Sokolov's systems may come from divergences in the strength of polymer−substrate interactions. It has strong hydrogen-bonding interactions occurring between poly(vinyl acetate), P2VP, and $SiO_2$, while the interfacial interactions in our system (i.e., $\pi-\pi$ interactions) are relatively weaker. The stronger interfacial interactions between P2VP and $SiO_2$ promote adsorption and dense packing of chains at the interface and presumably induce large variations in chain-packing density as $M_w$ is altered, and as a result, chain packing at the interface becomes important. As well, the different length scales of polymer dynamics probed (segment relaxation vs chain diffusion) may also result in the different $M_w$ effects. Despite the controversies, our results, taking into account the propagation depth of the interfacial dynamics, provide alternative insight into the $M_w$-dependent interfacial effect of nanoconfined polymers.

## CONCLUSIONS

In this paper, we characterized the effective viscosity of supported PS thin films with various molecular weights on phenyl group-modified substrates by probing the growth dynamics of the "*wetting ridge*". The distance from a solid substrate over which polymer dynamics are suppressed was assessed by measuring the vertical diffusion of fluorinated tracer-labeled polymer chains in a bilayer film. We found that the viscosity of PS thin films increased because of the $\pi-\pi$ interactions at the polymer−substrate interface. PS thin films with higher $M_w$ and supported by substrates with larger amounts of phenyl groups exhibited a much more pronounced viscosity increase. Concurrently, the utmost distance of dynamics suppression by the interacting substrate ($h_c^*$) increased with an increased $M_w$ of PS and amount of phenyl groups on the substrate. Furthermore, we revealed that the viscosity data for all the samples collapsed into a linear line if we plot the increase in viscosity, represented by $\eta_{film}/\eta_{bulk}$, due to the interfacial effect against $h_c^*$. This result clearly suggests that the interfacial effect can be qualitatively scaled by the distance over which the suppression of substrate dynamics propagates.

These results enabled us to achieve an additional understanding on the molecular weight-dependence of the interfacial effect. The suppressed interfacial dynamics can be extended over a longer distance from the substrate interface within a film having larger $M_w$, and therefore is associated with a greater increase in viscosity and more substantial mobility reductions.

## ASSOCIATED CONTENT

### Supporting Information

The Supporting Information is available free of charge on the ACS Publications website at DOI: 10.1021/acs.macromol.9b00226.

Contact angle, XPS, and SFG spectra of PTS-modified substrate (PDF)

## AUTHOR INFORMATION


### Corresponding Authors

*E-mail: chemizuo@zstu.edu.cn (B.Z.).
*E-mail: wxinping@yahoo.com, wxinping@zstu.edu.cn (X.W.).

### ORCID

Biao Zuo: 0000-0002-4921-8823
Rodney D. Priestley: 0000-0001-6765-2933
Xinping Wang: 0000-0002-9269-3275


### Notes

The authors declare no competing financial interest.

## ACKNOWLEDGMENTS

We are thankful for financial support from the National Natural Science Foundation of China (NSFC, 21504081, 21674100, 21873085) and China Scholarship Council and the National Science Foundation (NSF) Materials Research Science and Engineering Center Program through the Princeton Center for Complex Materials (DMR-1420541). R.D.P. acknowledges the NSF through CBET—1706012.



DOI: 10.1021/acs.macromol.9b00226
*Macromolecules* 2019, 52, 3753−3762

## REFERENCES


(1) Keddie, J. L.; Jones, R. A. L.; Cory, R. A. Size-Dependent Depression of the Glass Transition Temperature in Polymer Films. *Europhys. Lett.* **1994**, *27*, 59−64.

(2) Sharp, J. S.; Forrest, J. A. Free Surfaces Cause Reductions in the GlassTransition Temperature of Thin Polystyrene Films. *Phys. Rev. Lett.* **2003**, *91*, 235701.

(3) Ellison, C. J.; Torkelson, J. M. The Distribution of Glass-transition Temperatures in Nanoscopically Confined Glass Formers. *Nat. Mater.* **2003**, *2*, 695−700.

(4) Zuo, B.; Liu, Y.; Liang, Y.; Kawaguchi, D.; Tanaka, K.; Wang, X. Glass Transition Behavior in Thin Polymer Films Covered with a Surface Crystalline Layer. *Macromolecules* **2017**, *50*, 2061−2068.

(5) Oh, H.; Green, P. F. Polymer Chain Dynamics and Glass Transition in Athermal Polymer/nanoparticle Mixtures. *Nat. Mater.* **2009**, *8*, 139−143.

(6) Zhang, C.; Guo, Y.; Priestley, R. D. Glass Transition Temperature of Polymer Nanoparticles under Soft and Hard Confinement. *Macromolecules* **2011**, *44*, 4001−4006.

(7) Rowland, H. D.; King, W. P.; Pethica, J. B.; Cross, G. L. W. Molecular Confinement Accelerates Deformation of Entangled Polymers During Squeeze Flow. *Science* **2008**, *322*, 720−724.

(8) Chen, F.; Peng, D.; Ogata, Y.; Tanaka, K.; Yang, Z.; Fujii, Y.; Yamada, N. L.; Lam, C.-H.; Tsui, O. K. C. Confinement Effect on the Effective Viscosity of Plasticized Polymer Films. *Macromolecules* **2015**, *48*, 7719−7726.

(9) O'Connell, P. A.; McKenna, G. B. Rheological Measurements of the Thermo- viscoelastic Response of Ultrathin Polymer Films. *Science* **2005**, *307*, 1760−1763.

(10) Chowdhury, M.; Guo, Y.; Wang, Y.; Merling, W. L.; Mangalara, J. H.; Simmons, D. S.; Priestley, R. D. Spatially Distributed Rheological Properties in Confined Polymers by Noncontact Shear. *J. Phys. Chem. Lett.* **2017**, *8*, 1229−1234.

(11) Pu, Y.; Rafailovich, M. H.; Sokolov, J.; Gersappe, D.; Peterson, T.; Wu, W.-L.; Schwarz, S. A. Mobility of Polymer Chains Confined at a Free Surface. *Phys. Rev. Lett.* **2001**, *87*, 206101.

(12) Frank, B.; Gast, A. P.; Russell, T. P.; Brown, H. R.; Hawker, C. Polymer Mobility in Thin Films. *Macromolecules* **1996**, *29*, 6531−6534.

(13) Katsumata, R.; Dulaney, A. R.; Kim, C. B.; Ellison, C. J. Glass Transition and Self-Diffusion of Unentangled Polymer Melts Nanoconfined by Different Interfaces. *Macromolecules* **2018**, *51*, 7509−7517.

(14) Zheng, X.; Rafailovich, M. H.; Sokolov, J.; Strzhemechny, Y.; Schwarz, S. A.; Sauer, B. B.; Rubinstein, M. Long-Range Effects on Polymer Diffusion Induced by a Bounding Interface. *Phys. Rev. Lett.* **1997**, *79*, 241−244.

(15) Keddie, J. L.; Jones, R. A. L.; Cory, R. A. Interface and Surface Effects on the Glass-transition Temperature in Thin Polymer Films. *Faraday Discuss.* **1994**, *98*, 219−230.

(16) Zheng, F.; Zuo, B.; Zhu, Y.; Yang, J.; Wang, X. Probing Substrate Effects on Relaxation Dynamics of Ultrathin Poly(vinyl acetate) Films by Dynamic Wetting of Water Droplets on Their Surfaces. *Soft Matter* **2013**, *9*, 11680−11689.

(17) Tsui, O. K. C.; Russell, T. P.; Hawker, C. J. Effect of Interfacial Interactions on the Glass Transition of Polymer Thin Films. *Macromolecules* **2001**, *34*, 5535−5539.

(18) Zhang, C.; Fujii, Y.; Tanaka, K. Effect of Long Range Interactions on the Glass Transition Temperature of Thin Polystyrene Films. *ACS Macro Lett.* **2012**, *1*, 1317−1320.

(19) Torres, J. A.; Nealey, P. F.; de Pablo, J. J. Molecular Simulation of Ultrathin Polymeric Films near the Glass Transition. *Phys. Rev. Lett.* **2000**, *85*, 3221−3224.

(20) Kim, C.; Facchetti, A.; Marks, T. J. Probing the Surface Glass Transition Temperature of Polymer Films via Organic Semiconductor Growth Mode, Microstructure, and Thin-Film Transistor Response. *J. Am. Chem. Soc.* **2009**, *131*, 9122−9132.

(21) Fryer, D. S.; Peters, R. D.; Kim, E. J.; Tomaszewski, J. E.; de Pablo, J. J.; Nealey, P. F.; White, C. C.; Wu, W.-l. Dependence of the Glass Transition Temperature of Polymer Films on Interfacial Energy and Thickness. *Macromolecules* **2001**, *34*, 5627−5634.

(22) Zuo, B.; Qian, C.; Yan, D.; Liu, Y.; Liu, W.; Fan, H.; Tian, H.; Wang, X. Probing Glass Transitions in Thin and Ultrathin Polystyrene Films by Stick-Slip Behavior during Dynamic Wetting of Liquid Droplets on Their Surfaces. *Macromolecules* **2013**, *46*, 1875−1882.

(23) Napolitano, S.; Wübbenhorst, M. The Lifetime of the Deviations from Bulk Behavior in Polymers Confned at the Nanoscale. *Nat. Commun.* **2011**, *2*, 260.

(24) Napolitano, S.; Sferrazza, M. How Irreversible Adsorption Affects Interfacial Properties of Polymers. *Adv. Colloid Interface Sci.* **2017**, *247*, 172−177.

(25) Napolitano, S.; Capponi, S.; Vanroy, B. Glassy Dynamics of Soft Matter under 1D Confinement: How Irreversible Adsorption Affects Molecular Packing, Mobility Gradients and Orientational Polarization in Thin Films. *Eur. Phys. J. E* **2013**, *36*, 61.

(26) Napolitano, S.; Glynos, E.; Tito, N. B. Glass transition of polymers in bulk, confined geometries, and near interfaces. *Rep. Prog. Phys.* **2017**, *80*, 036602.

(27) Koga, T.; Jiang, N.; Gin, P.; Endoh, M. K.; Narayanan, S.; Lurio, L. B.; Sinha, S. K. Impact of an Irreversibly Adsorbed Layer on Local Viscosity of Nanoconfined Polymer Melts. *Phys. Rev. Lett.* **2011**, *107*, 225901.

(28) Wang, H.; Hor, J. L.; Zhang, Y.; Liu, T.; Lee, D.; Fakhraai, Z. Dramatic Increase in Polymer Glass Transition Temperature under Extreme Nanoconfinement in Weakly Interacting Nanoparticle Films. *ACS Nano* **2018**, *12*, 5580−5587.

(29) Moll, J.; Kumar, S. K. Glass Transitions in Highly Attractive Highly Filled Polymer Nanocomposites. *Macromolecules* **2012**, *45*, 1131−1135.

(30) Holt, A. P.; Griffin, P. J.; Bocharova, V.; Agapov, A. L.; Imel, A. E.; Dadmun, M. D.; Sangoro, J. R.; Sokolov, A. P. Dynamics at the Polymer/Nanoparticle Interface in Poly(2-vinylpyridine)/Silica Nanocomposites. *Macromolecules* **2014**, *47*, 1837−1843.

(31) Holt, A. P.; Sangoro, J. R.; Wang, Y.; Agapov, A. L.; Sokolov, A. P. Chain and Segmental Dynamics of Poly(2-vinylpyridine) Nanocomposites. *Macromolecules* **2013**, *46*, 4168−4173.

(32) Huang, X.; Roth, C. B. Optimizing the Grafting Density of Tethered Chains to Alter the Local Glass Transition Temperature of Polystyrene near Silica Substrates: The Advantage of Mushrooms over Brushes. *ACS Macro Lett.* **2018**, *7*, 269−274.

(33) Lee, H.; Sethuraman, V.; Kim, Y.; Lee, W.; Ryu, D. Y.; Ganesan, V. Nonmonotonic Glass Transition Temperature of Polymer Films Supported on Polymer Brushes. *Macromolecules* **2018**, *51*, 4451−4461.

(34) Lee, H.; Ahn, H.; Naidu, S.; Seong, B. S.; Ryu, D. Y.; Trombly, D. M.; Ganesan, V. Glass Transition Behavior of PS Films on Grafted PS Substrates. *Macromolecules* **2010**, *43*, 9892−9898.

(35) Cheng, S.; Holt, A. P.; Wang, H.; Fan, F.; Bocharova, V.; Martin, H.; Etampawala, T.; White, B. T.; Saito, T.; Kang, N.-G.; Dadmun, M. D.; Mays, J. W.; Sokolov, A. P. Unexpected Molecular Weight Effect in Polymer Nanocomposites. *Phys. Rev. Lett.* **2016**, *116*, 038302.

(36) Voylov, D. N.; Holt, A. P.; Doughty, B.; Bocharova, V.; Meyer, H. M.; Cheng, S.; Martin, H.; Dadmun, M.; Kisliuk, A.; Sokolov, A. P. Unraveling the Molecular Weight Dependence of Interfacial Interactions in Poly(2-vinylpyridine)/Silica Nanocomposites. *ACS Macro Lett.* **2017**, *6*, 68−72.

(37) Sun, S.; Xu, H.; Han, J.; Zhu, Y.; Zuo, B.; Wang, X.; Zhang, W. The Architecture of the Adsorbed Layer at the Substrate Interface Determines the Glass Transition of Supported Ultrathin Polystyrene Films. *Soft Matter* **2016**, *12*, 8348−8358.

(38) Klonos, P.; Kulyk, K.; Borysenko, M. V.; Gun'ko, V. M.; Kyritsis, A.; Pissis, P. Effects of Molecular Weight below the Entanglement Threshold on Interfacial Nanoparticles/Polymer Dynamics. *Macromolecules* **2016**, *49*, 9457−9473.

(39) Yin, H.; Cangialosi, D.; Schönhals, A. Glass Transition and Segmental Dynamics in thin Supported Polystyrene Films: The Role




DOI: 10.1021/acs.macromol.9b00226
*Macromolecules* 2019, 52, 3753−3762

of Molecular Weight and Annealing. *Thermochim. Acta* **2013**, *566*, 186−192.
(40) Zuo, B.; Inutsuka, M.; Kawaguchi, D.; Wang, X.; Tanaka, K. Conformational Relaxation of Poly(styrene-co-butadiene) Chains at Substrate Interface in Spin-Coated and Solvent-Cast Films. *Macromolecules* **2018**, *51*, 2180−2186.
(41) Jeong, H.; Napolitano, S.; Arnold, C. B.; Priestley, R. D. Irreversible Adsorption Controls Crystallization in Vapor-Deposited Polymer Thin Films. *J. Phys. Chem. Lett.* **2017**, *8*, 229−234.
(42) Panagopoulou, A.; Napolitano, S. Irreversible Adsorption Governs the Equilibration of Thin Polymer Films. *Phys. Rev. Lett.* **2017**, *119*, 097801.
(43) Li, L.; Zhou, D.; Huang, D.; Xue, G. Double Glass Transition Temperatures of Poly(methyl methacrylate) Confined in Alumina Nanotube Templates. *Macromolecules* **2014**, *47*, 297−303.
(44) Harton, S. E.; Kumar, S. K.; Yang, H.; Koga, T.; Hicks, K.; Lee, H.; Mijovic, J.; Liu, M.; Vallery, R. S.; Gidley, D. W. Immobilized Polymer Layers on Spherical Nanoparticles. *Macromolecules* **2010**, *43*, 3415−3421.
(45) Chen, J.; Li, L.; Zhou, D.; Wang, X.; Xue, G. Effect of Geometric Curvature on Vitrification Behavior for Polymer Nanotubes Confined in Anodic Aluminum Oxide Templates. *Phys. Rev. E: Stat., Nonlinear, Soft Matter Phys.* **2015**, *92*, 032306.
(46) Gin, P.; Jiang, N.; Liang, C.; Taniguchi, T.; Akgun, B.; Satija, S. K.; Endoh, M. K.; Koga, T. Revealed Architectures of Adsorbed Polymer Chains at Solid-Polymer Melt Interfaces. *Phys. Rev. Lett.* **2012**, *109*, 265501.
(47) Jiang, N.; Shang, J.; Di, X.; Endoh, M. K.; Koga, T. Formation Mechanism of High-Density, Flattened Polymer Nanolayers Adsorbed on Planar Solids. *Macromolecules* **2014**, *47*, 2682−2689.
(48) Housmans, C.; Sferrazza, M.; Napolitano, S. Kinetics of Irreversible Chain Adsorption. *Macromolecules* **2014**, *47*, 3390−3393.
(49) He, Q.; Narayanan, S.; Wu, D. T.; Foster, M. D. Confinement Effects with Molten Thin Cyclic Polystyrene Films. *ACS Macro Lett.* **2016**, *5*, 999−1003.
(50) Siretanu, I.; Chapel, J. P.; Drummond, C. Substrate Remote Control of Polymer Film Surface Mobility. *Macromolecules* **2012**, *45*, 1001−1005.
(51) Zuo, B.; Xu, J.; Sun, S.; Liu, Y.; Yang, J.; Zhang, L.; Wang, X. Stepwise Crystallization and the Layered Distribution in Crystallization Kinetics of Ultra-Thin Poly(ethylene terephthalate) Film. *J. Chem. Phys.* **2016**, *144*, 234902.
(52) Jiang, N.; Sendogdular, L.; Di, X.; Sen, M.; Gin, P.; Endoh, M. K.; Koga, T.; Akgun, B.; Dimitriou, M.; Satija, S. Effect of CO2 on a Mobility Gradient of Polymer Chains near an Impenetrable Solid. *Macromolecules* **2015**, *48*, 1795−1803.
(53) Xu, J.; Liu, Z.; Lan, Y.; Zuo, B.; Wang, X.; Yang, J.; Zhang, W.; Hu, W. Mobility Gradient of Poly(ethylene terephthalate) Chains near a Substrate Scaled by the Thickness of the Adsorbed Layer. *Macromolecules* **2017**, *50*, 6804−6812.
(54) Perez-de-Eulate, N. G.; Sferrazza, M.; Cangialosi, D.; Napolitano, S. Irreversible Adsorption Erases the Free Surface Effect on the Tg of Supported Films of Poly(4-tert-butylstyrene). *ACS Macro Lett.* **2017**, *6*, 354−358.
(55) Xu, J.; Zhang, Y.; Zhou, H.; Hong, Y.; Zuo, B.; Wang, X.; Zhang, L. Probing the Utmost Distance of Polymer Dynamics Suppression by a Substrate by Investigating the Diffusion of Fluorinated Tracer-Labeled Polymer Chains. *Macromolecules* **2017**, *50*, 5905−5913.
(56) Zuo, B.; Tian, H.; Liang, Y.; Xu, H.; Zhang, W.; Zhang, L.; Wang, X. Probing the Rheological Properties of Supported Thin Polystyrene Films by Investigating the Growth Dynamics of Wetting Ridges. *Soft Matter* **2016**, *12*, 6120−6131.
(57) Yang, J.; Yuan, D.; Zhou, B.; Gao, J.; Ni, H.; Zhang, L.; Wang, X. Studies on the effects of the alkyl group on the surface segregation of poly(n-alkyl methacrylate) end-capped 2-perfluorooctylethyl methacrylate films. *J. Colloid Interface Sci.* **2011**, *359*, 269−278.
(58) Ni, H.; Li, X.; Hu, Y.; Zuo, B.; Zhao, Z.; Yang, J.; Yuan, D.; Ye, X.; Wang, X. Surface Structure of Spin-coated Fluorinated Polymers Films Dominated by Corresponding Film-formation Solution/air Interface Structure. *J. Phys. Chem. C* **2012**, *116*, 24151−24160.
(59) Huang, C.; Katz, H. E.; West, J. E. Solution-Processed Organic Field-Effect Transistors and Unipolar Inverters Using Self-Assembled Interface Dipoles on Gate Dielectrics. *Langmuir* **2007**, *23*, 13223−13231.
(60) Cassie, A. B. D. Contact Angles. *Discuss. Faraday Soc.* **1948**, *3*, 11−16.
(61) Hong, Y.; Li, Y.; Wang, F.; Zuo, B.; Wang, X.; Zhang, L.; Kawaguchi, D.; Tanaka, K. Enhanced Thermal Stability of Polystyrene by Interfacial Noncovalent Interactions. *Macromolecules* **2018**, *51*, 5620−5627.
(62) Lu, H.; Chen, W.; Russell, T. P. Relaxation of Thin Films of Polystyrene Floating on Ionic Liquid Surface. *Macromolecules* **2009**, *42*, 9111−9117.
(63) Carré, A.; Gastel, J.-C.; Shanahan, M. E. R. Viscoelastic Effects in the Spreading of Liquids. *Nature* **1996**, *379*, 432−434.
(64) Shanahan, M. E. R.; Carré, A. Spreading and Dynamics of Liquid Drops Involving Nanometric Deformations on Soft Substrates. *Colloids Surf., A* **2002**, *206*, 115−123.
(65) Shuto, K.; Oishi, Y.; Kajiyama, T.; Han, C. C. Preparation of 2-Dimensional Ultra Thin Polystyrene Film by Water Casting Method. *Polym. J.* **1993**, *25*, 291−300.
(66) Ferry, J. D. *Viscoelastic Properties of Polymers*, 3rd ed.; Wiley: New York, 1980.
(67) Alcoutlabi, M.; McKenna, G. B. Effects of Confinement on Material Behaviour at the Nanometre Size Scale. *J. Phys.: Condens. Matter* **2005**, *17*, R461−R524.
(68) Peng, D.; Yang, Z.; Tsui, O. K. C. Method To Measure the Viscoelastic Properties of Nanometer Entangled Polymer Films. *Macromolecules* **2011**, *44*, 7460−7464.
(69) Plazek, D. J.; Zheng, X. D.; Ngai, K. L. Viscoelastic properties of amorphous polymers. I. Different temperature dependences of segmental relaxation and terminal dispersion. *Macromolecules* **1992**, *25*, 4920−4924.
(70) Masson, J.-L.; Green, P. F. Viscosity of Entangled Polystyrene Thin Film Melts: Film Thickness Dependence. *Phys. Rev. E: Stat., Nonlinear, Soft Matter Phys.* **2002**, *65*, 031806.
(71) Jiang, N.; Endoh, M. K.; Koga, T. "Marker" grazing-incidence X-ray photon correlation spectroscopy: a new tool to peer into the interfaces of nanoconfined polymer thin films. *Polym. J.* **2013**, *45*, 26−33.
(72) Chen, F.; Peng, D.; Lam, C.-H.; Tsui, O. K. C. Viscosity and Surface-Promoted Slippage of Thin Polymer Films Supported by a Solid Substrate. *Macromolecules* **2015**, *48*, 5034−5039.
(73) Geng, K.; Tsui, O. K. C. Effects of Polymer Tacticity and Molecular Weight on the Glass Transition Temperature of Poly(methyl methacrylate) Films on Silica. *Macromolecules* **2016**, *49*, 2671−2678.
(74) Li, C.; Kim, H.; Jiang, J.; Li, C.; Koga, T.; Lurio, L.; Schwarz, S.; Narayanan, S.; Lee, H.; Lee, Y. J.; Jiang, Z.; Sinha, S.; Rafailovich, M. H.; Sokolov, J. C. The effect of Surface Interactions on the Viscosity of Polymer Thin Films. *Europhys. Lett.* **2006**, *73*, 899−905.
(75) Li, R. N.; Chen, F.; Lam, C.-H.; Tsui, O. K. C. Viscosity of PMMA on Silica: Epitome of Systems with Strong Polymer-Substrate Interactions. *Macromolecules* **2013**, *46*, 7889−7893.
(76) Mattsson, J.; Forrest, J. A.; Börjesson, L. Quantifying Glass Transition Behavior in Ultrathin Free-standing Polymer Films. *Phys. Rev. E: Stat. Phys., Plasmas, Fluids, Relat. Interdiscip. Top.* **2000**, *62*, 5187.
(77) Forrest, J. A.; Mattsson, J. Reductions of the Glass Transition Temperature in Thin Polymer Films: Probing the Length Scale of Cooperative Dynamics. *Phys. Rev. E: Stat. Phys., Plasmas, Fluids, Relat. Interdiscip. Top.* **2000**, *61*, R53.
(78) DeMaggio, G. B.; Frieze, W. E.; Gidley, D. W.; Zhu, M.; Hristov, H. A.; Yee, A. F. Interface and Surface Effects on the Glass Transition in Thin Polystyrene Films. *Phys. Rev. Lett.* **1997**, *78*, 1524−1527.


DOI: 10.1021/acs.macromol.9b00226
*Macromolecules* 2019, 52, 3753−3762

(79) Papon, A.; Montes, H.; Hanafi, M.; Lequeux, F.; Guy, L.; Saalwachter, K. Glass-transition Temperature Gradient in Nanocomposites: Evidence from Nuclear Magnetic Resonance and Differential Scanning cCalorimetry. *Phys. Rev. Lett.* **2012**, *108*, 065702.
(80) Starr, F. W.; Douglas, J. F.; Meng, D.; Kumar, S. K. Bound Layers "Cloak" Nanoparticles in Strongly Interacting Polymer Nanocomposites. *ACS Nano* **2016**, *10*, 10960−10965.
(81) Zhang, W.; Douglas, J. F.; Starr, F. W. Why We Need to Look beyond the Glass Transition Temperature to Characterize the Dynamics of Thin Supported Polymer Films. *Proc. Natl. Acad. Sci. U.S.A.* **2018**, *115*, 5641−5646.
(82) Yu, X.; Yiu, P.; Weng, L.-T.; Chen, F.; Tsui, O. K. C. Effective Viscosity of Lightly UVO-Treated Polystyrene Films on Silicon with Different Molecular Weights. *Macromolecules* **2019**, *52*, 877−885.
(83) Simavilla, D. N.; Huang, W.; Housmans, C.; Sferrazza, M.; Napolitano, S. Taming the Strength of Interfacial Interactions via Nanoconfinement. *ACS Cent. Sci.* **2018**, *4*, 755−759.



DOI: 10.1021/acs.macromol.9b00226
*Macromolecules* 2019, 52, 3753−3762